Cryostratigraphic record of permafrost degradation and recovery following historic surface disturbances, Klondike area, Yukon

F. Calmels[1] and D.G. Froese[2]
Deptartment of Earth and Atmospheric Sciences, University of Alberta[3]

Calmels, F. and Froese, D.G., 2009. Cryostratigraphic record of permafrost degradation and recovery following historic surface disturbances, Klondike area, Yukon. *In:* Yukon Exploration and Geology 2008, L.H. Weston, L.R. Blackburn and L.L. Lewis (eds.), Yukon Geological Survey, p. 85-97.

ABSTRACT

Cryostratigraphic investigation of near-surface permafrost at a site in the southern Klondike goldfields has revealed three ages of permafrost disturbance and recovery which potentially span the last century. In an undisturbed forest, the base of the modern active layer is stable with a suspended ice/sediment cryofacies at the contact. A recently burned site (2004) shows that the degrading contact has not yet stabilized. An earlier disturbance from the 1970s shows evidence of aggradation (upward shift) of the permafrost table following limited vegetation succession. Underlying all three sites is an older disturbance corresponding to a thaw depth of ~2 m, predating the 1970s disturbance; it is likely that this represents an early 20th century disturbance associated with the deforestation of the valley during the gold rush era. Permafrost has recovered significantly since that time as the boreal forest and understory vegetation was re-established, underscoring the role of vegetation cover in permafrost disturbance and recovery.

RÉSUMÉ

Une étude cryostratigraphique du pergélisol peu profond des champs aurifères du sud du Klondike dévoile trois périodes de dégradation et de récupération du permafrost durant le vingtième siècle. Le contact actuel du pergélisol avec la couche active dans une forêt non perturbée est stable avec une cryostructure riche en glace. Un site récemment incendié (2004) a un contact typique díune dégradation active. Une perturbation datant des années 1970 montre une récupération du pergélisol après reprise de la végétation. Les trois sites présentent une perturbation plus ancienne, antérieure aux années 1970, correspondant à un dégel ayant atteint ~2 m de profondeur. Cet accroissement important de la couche active résulte probablement díune perturbation liée à la déforestation de la vallée durant la ruée vers líor, au début du vingtième siècle. Le pergélisol a significativement récupéré depuis, avec la reprise de la forêt boréale et de la végétation basse. Cette reconstitution des événements souligne le rôle du couvert végétal dans la perturbation et la récupération du pergélisol.

[1]*fabrice.calmels@ualberta.ca*

[2]*duane.froese@ualberta.ca*

[3]*Edmonton, Alberta, Canada T6G 2E3, phone: 780-492-0017 fax: 780-480-2030*

INTRODUCTION

The potential impacts of future climate warming on permafrost are poorly understood. Several recent modelling efforts have predicted widespread melting-to-near-disappearance of permafrost in the coming century across much of the northern hemisphere (*e.g.* Lawrence and Slater, 2005). Seemingly inconsistent with these predictions is evidence for the long-term survival of permafrost within several metres of the surface for more than 700 000 years, a timeframe which includes past interglaciations that were warmer and of longer duration than the Holocene (Froese *et al.*, 2008). The presence of this ancient ice indicates that permafrost can survive in a warmer climate, but leaves open the question of how has it survived? And what properties of the overlying insulating cover of vegetation, sediment and ice contribute to its resilience?

This paper presents preliminary results of a cryostratigraphic characterization of Klondike permafrost where thermal disturbance occurred due to the removal of peat and vegetation cover following a recent fire, mining activities and deforestation over the past century. We use a new technique for permafrost characterization – computed tomography (CT) scanning – to image permafrost cores and establish the ice characteristics of the near-subsurface permafrost. This, in turn, allows us to interpret the dynamical history of permafrost over the last century and better understand degradation and subsequent aggradation of the permafrost table following re-establishment of vegetation cover.

The Klondike goldfields provide an exceptional site to study the dynamics of permafrost given that the area has been subject to several periods of disturbance from mining activities dating to the late 19th century. During the gold rush era (*ca.* 1896 to 1910) deforestation of valleys occurred to support the growing need for wood for a variety of uses, ranging from cribbing, flume and trestle construction, cabins, and melting of permafrost in shafts; as well, understory moss was collected in many areas for fuel, as well as a source to insulate cabins (Morse, 2003). Subsequently, with the transition to large-scale dredging after 1905, ground was stripped and thawed for gold recovery in valley bottoms (Green, 1977). In addition to the areas that were mined, disturbances resulted from industrial development: roads, railways, telegraph lines and ditches were significant features developed during this era (Hogan and Skuce, 1992a, 1992b, 1993). Many of these sites were abandoned shortly after construction, but some persisted through the following half-century until large-scale mining largely ended in the 1960s (Green, 1977). More localized disturbances of areas that had not been affected by dredging occurred through the last 40 years. Furthermore, forest fires impacted large areas of the Klondike. This rich history of a hundred years of anthropogenic and natural permafrost disturbances provides the possibility to use these perturbations of varying age and severity to develop a model of permafrost degradation and recovery as an analogue for future climate change.

STUDY AREA

The Dominion Creek study area contains several sites with differing ages of disturbance within a few hundred square metres (Fig. 1). The original environment is a gently sloping (4-5°) pediment surface developed on loessal silts along the north side of the Dominion Creek valley. These loessal silts accumulated during the Pleistocene from the transport and deposition of wind-blown silt. Upslope, the surface grades into the colluvial mantle along the valley margin. The area was largely deforested during the early 20th century, as witnessed by the presence of stumps of mature trees in the recent-growth forest. As well, old-timer workings are present in the area, conspicuous from tailings piles and historic artefacts recovered by present-day mining (A. Sailer, pers. comm., 2008).

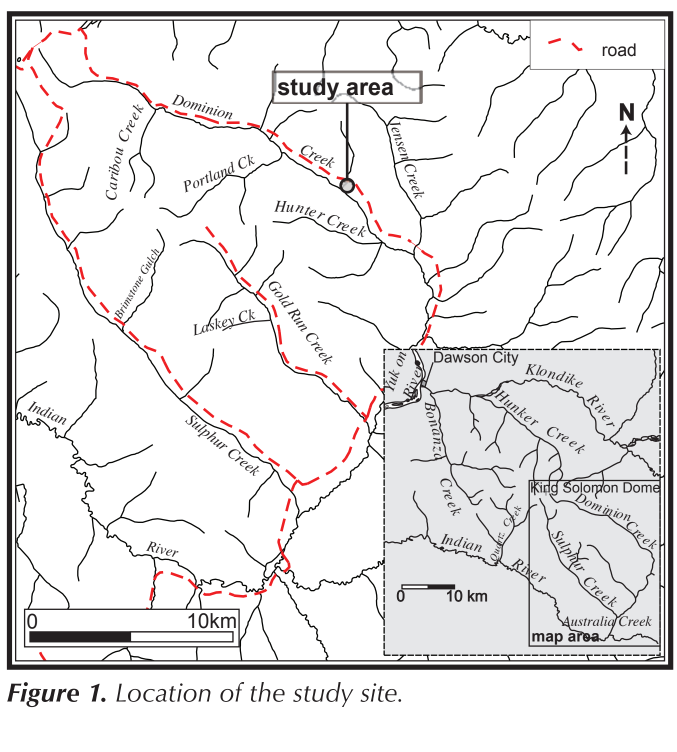

Figure 1. *Location of the study site.*

Mechanized mining at the site since the 1960s has generated several local disturbances of the surface vegetation cover. Three roads are present throughout the forest, where trees were cut or uprooted, and the peat cover was deeply compacted or perhaps ripped up by the tracks. Some ruts were created where surface water was channelled and has induced degradation of the permafrost. These road tracks are present in the woods of the studied area (Fig. 2a). In 2004, a large fire affected several areas of the Klondike along the Dominion Creek valley. One of the burned areas is along the same geomorphic surface adjacent to the road sites (Fig. 3). A combination of burning and bulldozer firebreaks disturbed the forest and provide three types of closely adjacent field conditions: (i) fire-disturbed areas where peat cover was removed (firebreak); (ii) fire-disturbed areas where peat cover persisted and only tree and shrub cover was affected (Fig. 2b); and (iii) undisturbed sites where forest cover was unaffected by the fire.

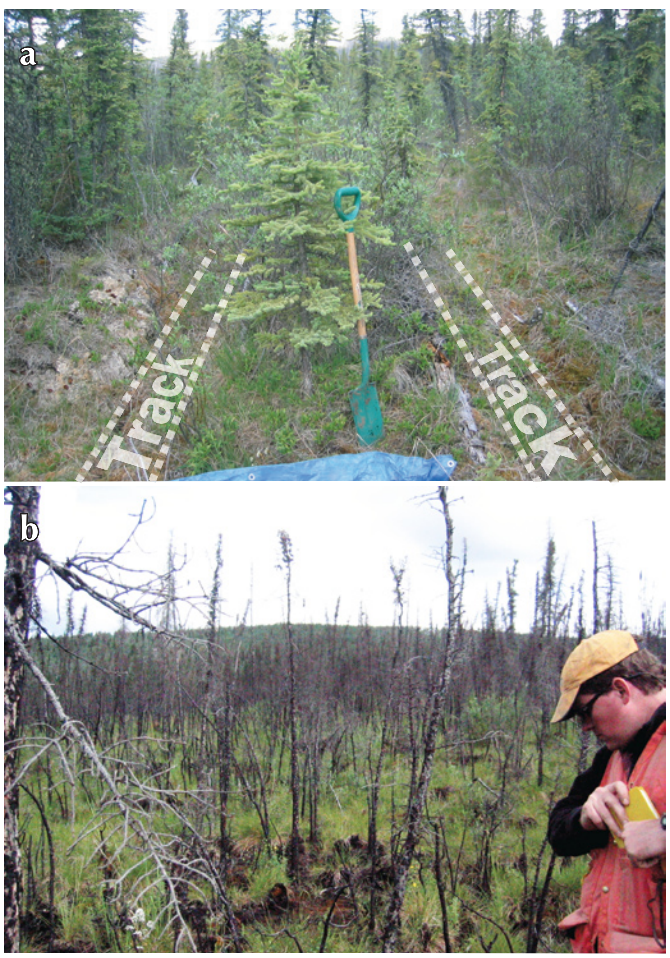

Figure 2. *Studied sites:* ***(a)*** *vehicle tracks; and* ***(b)*** *2004 fire.*

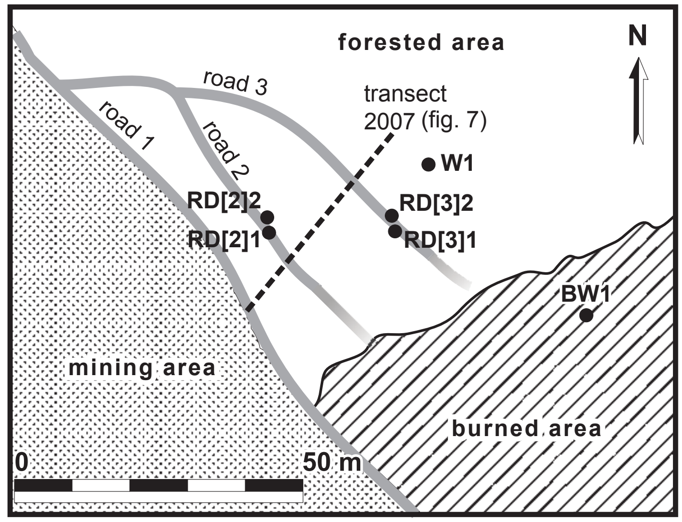

Figure 3. *Studied sites, active layer transect survey and borehole location.*

To summarize, three generations of degradation/recovery of permafrost are present: (i) a wooded area which recovered from deforestation, probably dating from the early 20th century; (ii) bulldozer tracks from the late 1960s to early 1970s where vegetation is still recovering from the disturbance; and (iii) burned areas associated with the 2004 fire where degradation is ongoing (Fig. 3).

METHODS

In order to understand the dynamics of permafrost and its recovery following disturbance, multiple techniques were used, including active layer probing to determine actual end of summer thaw depth, recovery of permafrost cores and CT scanning to determine the properties of shallow permafrost, and hand augering where permafrost was not encountered with the probe. As well, approximate ages of disturbances were confirmed with tree-ring analyses, dating from late 1960s to early 1970s.

ACTIVE LAYER PROBING

Active layer thickness is an important property in understanding permafrost dynamics and determining rates of degradation and recovery. Following a perturbation, permafrost thaws from the top and the active layer increases as the thermal disturbance extends further into the ground. Active layer depths were assessed in September 2007 using a graduated metal rod, inserted vertically into the ground until the permafrost was encountered. In July 2008, a hand auger was used to reach a depth of 5.10 m at sites where permafrost was not encountered.

SAMPLING

Six boreholes were drilled from early June to mid-July 2008 for permafrost sampling using a light, portable drill (see Calmels *et al*., 2005). Mounted on a small Stihl™ engine with a high-speed transmission, 1 m connecting steel rods terminate in a 10 cm diameter core barrel with a carbide bit with set diamonds. This system allowed cutting through isolated stones or even boulders, which would have not been possible with a conventional CRREL coring kit. Core sections were recovered, wrapped with plastic, stored frozen in a freezer and returned to the University of Alberta, Edmonton, Alberta, where they were untouched prior to CT scan imaging.

CORE IMAGING BY CT SCANNING

Imaging was done using a Toshiba Aquilion medical scanner at the Alberta Research Council in Edmonton, AB. Based on the principles of radiography, CT scanning (computed tomography scanning) provides a non-destructive examination of materials at the micro level, and provides imaging through mapping of density contrast. This technique allows a detailed interpretation down to the millimetre-scale of ice lenses, as well as individual gas bubbles and their orientation, in order to establish the processes that took place during freezing of the permafrost. Furthermore, diagenetic changes such as water migration, gas segregation in bubbles and cavities, and volume-change related deformations may be inferred. The advantages of CT scanning in permafrost studies are discussed in detail by Calmels and Allard (2004, 2008).

The Toshiba Aquilion medical scanner has a spatial resolution of 0.35 mm for transverse sections, and 0.5 mm for longitudinal sections. The cores were taken out of the freezer for the few minutes needed for the analyses and were otherwise kept in their sealed bags. The system produces a series of transverse slices (Fig. 4a). Medical software is used to process a 3-D reconstruction from the slices (Fig. 4b), and thereafter to extract any longitudinal sections across the slice series (Fig. 4c). Typically, images are in grey tones, showing the complete spectrum of densities; lower density materials appear in dark colours or tones, and higher density materials are expressed in light colours. Using image processing, it is also possible to select narrow ranges of the spectrum of density, so that it is possible to image selected components individually (*i.e.* ice, gas or soil). Ultimately, the ice and gas volumetric contents can be estimated from the CT scan images using medical imaging software such as Osiris™.

RESULTS

ACTIVE LAYER SURVEY

Active layer probing in September 2007 showed that in undisturbed woods, where the peat cover was 36 cm thick, and the slope was gentle (4-5°), active layer thickness was about 42 cm (Fig. 5b). In the upper forested area, where the slope was steeper and the soil dryer, active layer thickness exceeded 150 cm (Fig. 5a). This largely reflects changes in moisture associated with the steeper slope resulting in a thinner peat cover and, as a result, a thinner insulating surface layer. In the area associated with the 2004 fire, the thaw front reached a depth of 85 to 86 cm, with or without the overlying peat

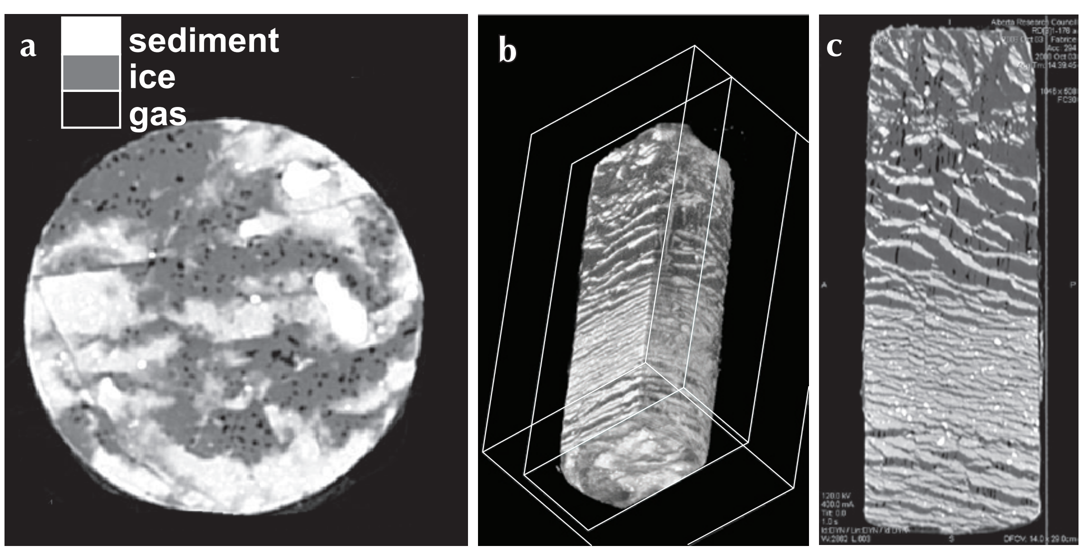

Figure 4. *Three modes of imaging scanner data. Core is 10 cm in diameter.* ***(a)*** *Transverse slice;* ***(b)*** *3-D reconstruction;* ***(c)*** *Longitudinal section. Soil is white, ice is grey and gas is black.*

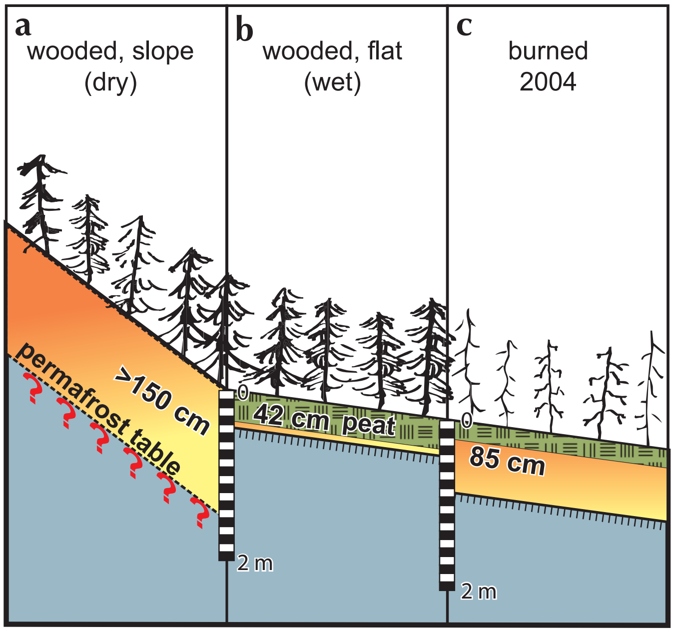

Figure 5. Active layer depths in wooded and fire disturbed areas.

cover (Fig. 5c). Where the peat remained, its surface was burned, and its average thickness was 20 cm or slightly less. In these degrading sites, the peat did not seem to have a major influence on ground thermal conditions. Due to the impact of the fire in the past three years, the active layer had approximately doubled from 42 to 86 cm, suggesting a melting rate of nearly 15 cm/year for the permafrost.

A second active-layer survey was completed 30 m outside of the 2004 burned area on the same geomorphic surface from the undisturbed wooded area (Fig. 6); it intersected three bulldozer trails dating back to the late 1960s to early 1970s. Each bulldozer trail consisted of two parallel tracks with a raised area in the middle. Active layer thicknesses ranged from 42 to 76 cm in the undisturbed wooded areas. The wooded area at road three has similar active layer thicknesses as those observed at the undisturbed wooded areas. On road two, the thawing front reached 86 cm. A more degraded road, road one, probably of the same origin and age as the other two roads has an active layer thickness of more than 170 cm. In July, 2008, additional probing with an auger was completed on road 1 to a depth of 5.1 m. The surface of road 1 was particularly wet, likely as a result of channelled surface runoff. Considering the present depth and the magnitude of permafrost table depth in the area, it is probable that the top of the permafrost is about six metres deep.

GEOCRYOSTRATIGRAPHIC OBSERVATIONS

The following section presents preliminary observations of ice and gas content within sampled core; sedimentary parameters are still being analysed. Six permafrost cores were recovered in the study area at W1, RD[2]1, RD[2]2, RD[3]1, RD[3]2, and BW1 (Fig. 3). In 2004, five boreholes W1, RD[2]1, RD[2]2, RD[3]1 and RD[3]2 were completed in the wooded, mainly undisturbed area, while a sixth, BW1, was located 36 m away in a burned area. The first five were collected in a line slightly oblique to the transect shown in Figure 6, which begins at the wooded area (borehole W1), crosses the bulldozer tracks on 'road three' (boreholes RD[3]1 and RD[3]2), and 'road two' (RD[2]1 and RD[2]2), and ends in the middle of the track on 'road one.'

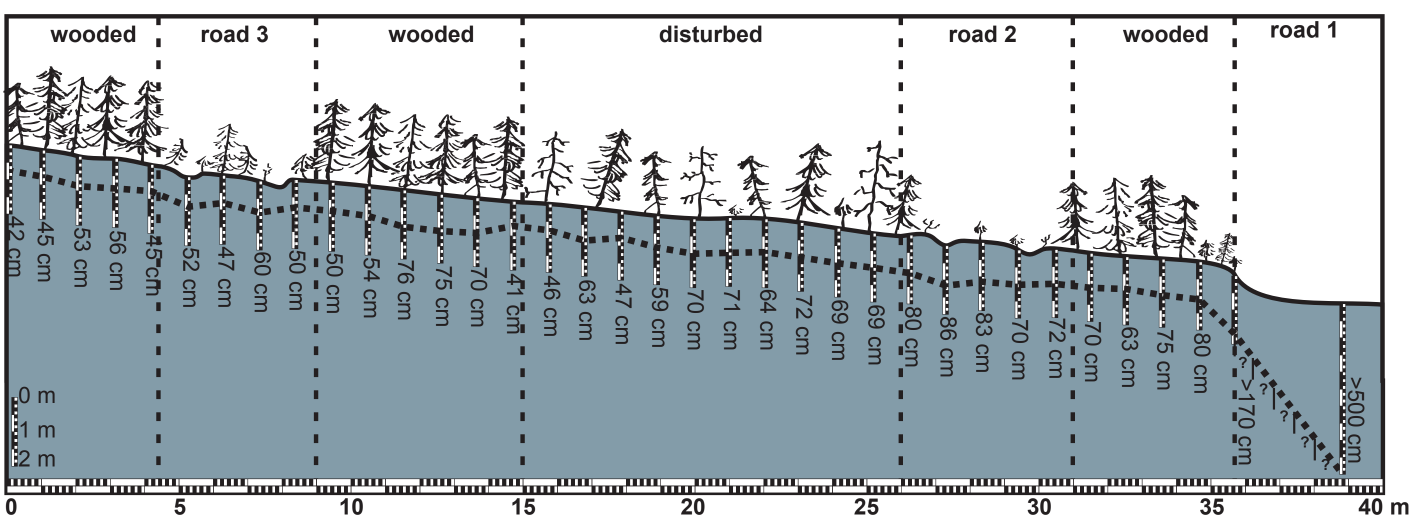

Figure 6. Active layer conditions in forested site along a transect crossing the 1970s roads.

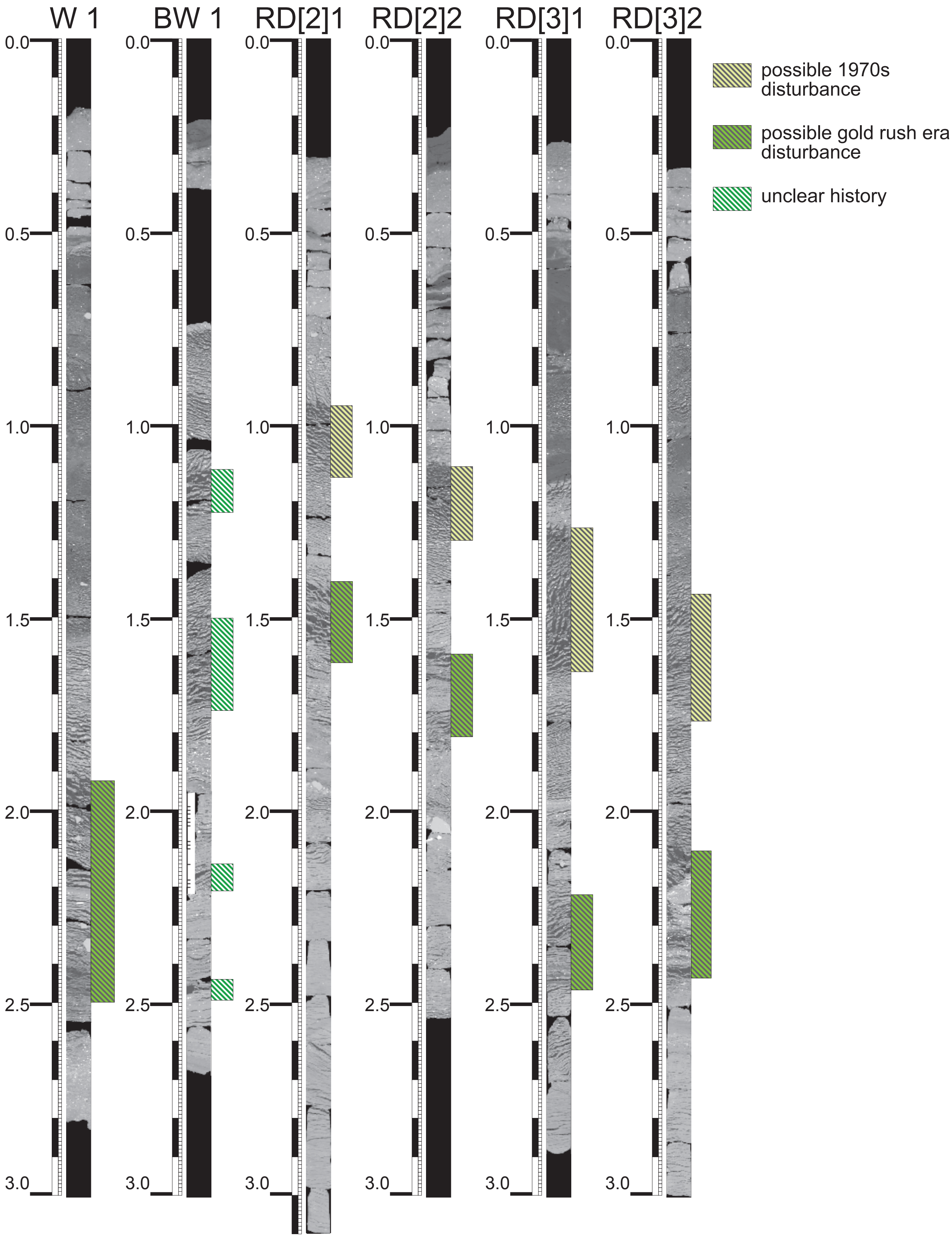

Figure 7. *Geocryological profiles of the cores for each site. Depth is in metres.*

Figure 7 shows the complete geocryological profiles of each core. It is important to note that the cores are not oriented. All of the cores share some geocryological similarities. The sedimentary and geomorphologic characteristics of the area provide a context for these shared features. The sediment is largely a sandy-silt with rare pebbles and coarse-sediment lenses. In the studied sites, the cryostructures are related mainly to segregational ice. When freezing progresses in mineral or organic soils, cryosuction causes the migration and subsequent freezing of pore water from the unfrozen soil to the freezing front, which results in the formation of discrete layers or lenses (Mackay, 1971; Williams, 1979; Gilpin, 1980; Williams and Smith, 1989; Konrad, 1990; IPA, 2005). This phenomenon, called ice segregation, is well developed in fine-grained sediments with good moisture availability. The segregation ice usually develops downward when permafrost progress from the surface, but can also form when the upper boundary surface of permafrost progresseses upward into the active layer, forming aggradational ice (French, 1996).

Cryostructures

Four main cryostructures are present in our geocryological profiles. We partially follow Murton and French (1994) in our classification; we do not consider structureless units and have added an organic-rich cryostructure to our classification system.

(i) Layered

A layered cryostructure is most commonly encountered in our cores (Fig. 8a). It consists of an alternation of continuous bands of ice with continuous sediment layers. As shown in Figure 7, the layered cryostructure is common in all cores and has ice-layer thicknesses ranging from <1 mm to 2 cm, with an average of 5 to 6 mm. The layering is subhorizontal and ice lensing is slightly tilted; even without orientation of the samples, we can reasonably assume that tilting is subparallel with, or influenced by, the slope, and freezing has propagated mainly parallel to the slope surface. Two forms of the layered cryostructures are observed: parallel wavy and non-parallel wavy.

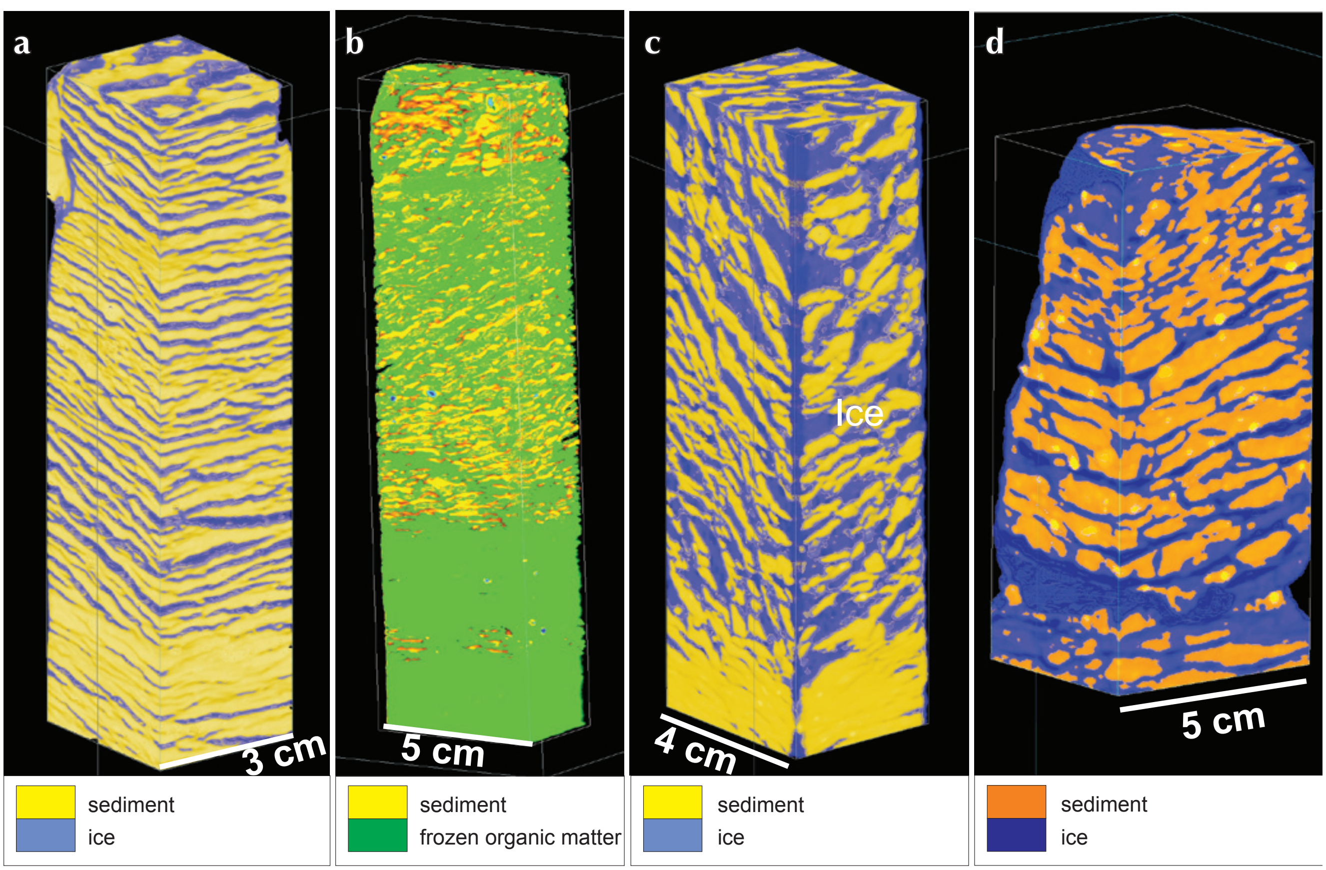

***Figure 8.** Cryostructures observed in boreholes revealed by CT scanning of permafrost cores: **(a)** layered; **(b)** organic rich; **(c)** suspended; and **(d)** reticulate.*

A layered cryostructure can be related to ice-wedges, segregational ice, intrusive ice, buried glaciers or ice bodies. At our sites, only ice segregation is involved in the genesis of this cryostructure. The combination of freezing rate and water availability influence ice-lensing and the thickness of the ice and sediment layers. The relatively thin ice layers suggest relatively modest water supply or a rapid freezing rate.

(ii) Organic-rich

Frozen organic-rich zones are encountered along some of our profiles (Fig. 8b). The organic-rich cryostructure is present in cores RD[3]1 from 50 to 115 cm, in RD[3]2 from ~65 to 130 cm, and to a lesser degree in W1 from 50 to 130 cm where the organic material is mixed within the sediment,. The organic-rich cryostructure is largely absent in cores BW1, RD[2]1 and RD[2]2. The proximity of sites RD[3]1, RD[3]1 and W1 suggests that this organic-rich zone is restricted to individual cores and does not represent a cryostructure with a great lateral extent. Several processes may produce the organic concentration, and its origin is not clear. The accumulation of organic matter may have formed when the surface of the site existed as a topographic depression or a small thermokarst pond where organic sedimentation took place. These zones are particularly ice rich due to their high porosity. Organic matter, such as peat, has a density similar to that of ice, and appears dark grey on CT scans. The frozen peat can be distinguished from pure ice by its mineral content, and it appears slightly brighter, with distinct sediment beds and lenses on CT scans.

(iii) Suspended

A suspended cryostructure is characterized by aggregates or sediment particles suspended in an ice matrix, with ice content exceeding sediment content (Fig. 8c). The suspended cryostructure is often encountered in massive ice and also in the uppermost 10 cm of permafrost (*i.e.* directly underlying the active layer, Mackay, 1972; Murton and French, 1994) where aggradational ice is forming (Yershov, 1998). In such conditions, the thermal gradient is low and ice lensing is fed by the perched water available on the permafrost table. In general, this type of cryostructure likely reflects a lower thermal regime favouring ice segregation, as well as greater water supply favouring segregational ice growth (Yershov, 1998).

In our cores, the cryostructures were not always homogeneous and show variation in ice content within a single cryostratigraphic unit. Ice lenses range from a few millimetres to 2 cm. The thickness of the cryostructure ranges from approximately 20 to 40 cm and is present in all cores. It is interesting to note that in our cores, the gas content is greatest in these thick ice layers. Generally, the gas content consists of elongated cylindrical bubbles extending from the sediment into the ice. The association of this gas feature with thick lenses of segregational ice suggests they could be characteristic of lower freezing rates.

(iv) Reticulate

A reticulate cryostructure consists of a three-dimensional network of vertical and horizontal ice veins isolating sediment blocks (Fig. 8d). It can be regular, containing rectangular or rhombic sediment blocks, or irregular containing irregularly shaped blocks. The structure is only encountered in BW1 core, from ~196 to 210 cm, and can be considered rare at our sites. This could reflect the low moisture content or other sediment properties in this particular location. Mackay (1974) suggests that reticulate ice veins grow in horizontal and vertical shrinkage cracks with much of the water coming from the adjacent material in a semi-closed freezing system, rather than from migration of water in an open system.

Cryostratigraphy of sites

The geocryological description of each site, with respect to their cryostructures, is presented below. The undisturbed site is described first, then the recently disturbed site, and finally the 1970s disturbed sites.

(i) W1, the forested site

W1 is a control site intended to represent an undisturbed, wooded site. Nevertheless, the presence of stumps and artefacts of the gold rush era in the area suggests it was disturbed in the early 20th century. Core W1 reaches a depth of 2.83 m. It has a surface cover of 5 cm of moss above 15 cm of humified peat. The thawing front was immediately below the organic layer in July 2008. Active layer samples have thin (1 mm or less) ice lenses in a sandy-silt matrix. The permafrost table was encountered at 51 to 58 cm depth, marked by an organic-rich zone where distinct ice lensing occurs below 58 cm (Fig. 9a). The diffuse nature of the upper boundary of the permafrost suggests a stable thermal equilibrium between the active layer and the permafrost table with few changes in recent time. This would indicate relatively constant surface conditions, with depth fluctuations of the permafrost being mainly controlled by climate. At a depth of approximately 150 cm, a fine, wavy layered cryostructure is present with millimetre-thick sediment

Figure 9. Cryostructures in core W1 (forested site): ***(a)*** upper boundary of permafrost; ***(b)*** layered cryostructure; and ***(c)*** suspended cryostructure.

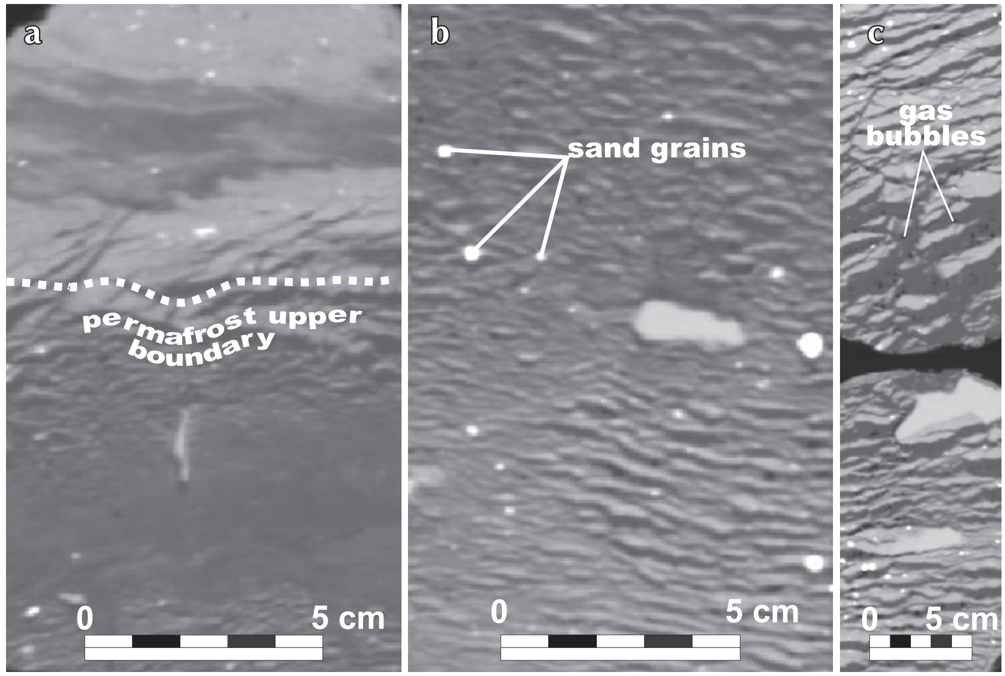

and ice layering (Fig. 9b). Below 150 cm, a larger layered cryostructure is present to a depth of 200 cm where it grades to a suspended structure with the highest ice content observed in the profile (Fig. 7, 9c). Below this zone, the cryostructure grades to layered and thinly layered/lenticular transitional facies to a depth of approximately 260 cm where ice lenses are rare to absent. Sand, pebble and clasts (up to ~7 cm) are present in a fine-grained sediment matrix. Overall, one very ice-rich zone (suspended cryostructure) is present at around 2 m depth, and the upper permafrost boundary suggests that no disturbance occurred during recent decades.

(ii) BW1, the 2004 burned site

Core BW1 was taken to a depth of 2.64 m and was collected to study the impact of the recent fire on the geocryological profile. The organic cover was burned and consists of an 8 cm-thick moss layer above 12 cm of dark humified peat. The thickness of the unfrozen ground at the time of sampling was 28 cm, including the organic cover. Active layer samples collected between 40 and 73 cm of depth were disturbed during the drilling process and were discarded. The permafrost table was noted at 76 cm, marked by a sharp contact (Fig. 10a, upper part), suggesting that the active layer is still increasing since the 2004 fire. The cryostructure is mainly non-parallel, wavy layered with tilted ice lenses (Fig 10a, lower part). Two major ice-rich zones include a suspended cryostructure at ~ 115 cm and 160 cm depth; two other minor ones are present at ~215 cm and 245 cm (Fig. 7). Usually, gas bubbles are observable within thick ice layers, but less common where ice lenses are thinner (Fig. 10b). Some beds of coarse particles are observed within the silty matrix. The orientation of this bed is tilted similar to the ice lensing (Fig. 10c), reflecting the general slope of the terrain. With the decrease in ice content with depth in the profile, other mixed cryostructures are observed such as the regular reticulate facies at 260 cm depth (Fig. 10d). Overall, two noticeable very ice-rich zones (suspended cryostructure) are present between 115 and 175 cm. The actual thaw discontinuity over the geocryological facies suggests that the active-layer thickness is still deepening in response to the 2004 fire disturbance.

(iii) RD[2]&[3], the late 1960s - early 1970s roads

The 'roads' are paths left by tracked vehicles in the early 1970s (A. Sailer, pers. comm., 2007), consisting of two depressed ruts separated by a higher, vegetated mound (Fig. 2a). Boreholes RD[2]1 and RD[3]1 were drilled in the ruts of the roads, whereas boreholes RD[2]2 and RD[3]2 were drilled in the vegetated mounds between the ruts to assess variability in the degradation and recovery processes.

Boreholes RD[2]1 and RD[2]2 have a depth of 3.09 and 2.54 m, respectively. The organic cover for both sites consists of 10 to 12 cm-thick moss cover above 15 cm of humified peat. The thawing front was directly below the organic layer between 27 and 30 cm, whereas the

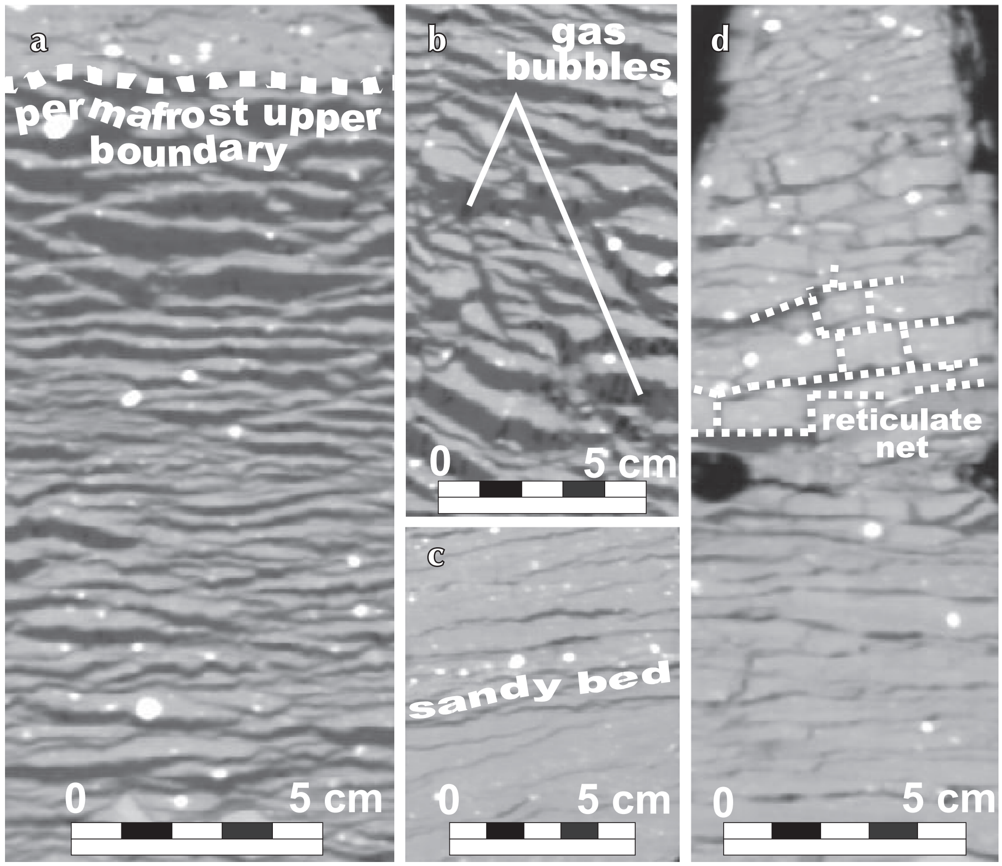

Figure 10. *Cryostructures in core BW1 (2004 burned site):* ***(a)*** *upper boundary of permafrost above wavy layered cryostructure;* ***(b)*** *suspended cryostructure;* ***(c)*** *sandy beds; and* ***(d)*** *reticulate cryostructure.*

permafrost table was at 95 and 110 cm for RD[2]1 and RD[2]2, respectively (Fig. 11a and 11b respectively). For both cores, the top of the modern permafrost table is ice rich and has a suspended cryostructure (Fig. 7, 11c). Some nearly vertical ice-veins propagate from the permafrost table into the active layer, probably due to the shrinkage of the sediment under the action of the cryodessication induced by the rising of the permafrost table (Mackay, 1972, 1974; Yershov, 1998; Williams, 1995). Below the upper permafrost boundary, the cryostructure is non-parallel wavy layered and is underlain by a lower ice-rich zone at 140 and 155 cm depth for RD[2]1 and RD[2]2, respectively (Fig. 7). Below these ice-rich zones, a layered cryostructure is present and the ice content decreases. Sand lenses, pebbles and small boulders occur infrequently in the profile, though distinct coarser layers are present at 192 and 208 cm for RD[2]1 and RD[2]2, respectively. The geocryological and sedimentary profiles of these two cores are consistent with a slight vertical offset of 15 cm, corresponding to the difference in surface profile between the ruts and the centre mound. RD[2] has two ice-rich zones at approximately 100 cm and 150 cm depth.

Cores RD[3]1 and RD[3]2 have depths of 2.84 and 2.99 m, respectively. The organic cover for both sites (27 cm for RD[3]1, 25 cm for RD[3]2) consists of a 6 to 8 cm-thick moss cover above 17 to 20 cm of humified peat. The thawing front was noted between 33 and 35 cm depth. The permafrost table was observed at 51 and 66 cm for RD[3]1 and RD[3]2, respectively, marked by a one centimetre-thick, sub-horizontal ice lens and vertical ice-veins above an organic-rich cryostructure. Some vertical ice veins are present in RD[2] cores and extend from the permafrost table; this zone is ice rich in both RD[2] and RD[1] cores. RD[2] cores have a higher organic content (Fig. 11d,e). The organic-rich level occurring just below the permafrost table probably prevented the formation of a suspended cryofacies. Below this depth, an ice-rich suspended cryostructure occurs at 130 (RD[3]1) and 145 cm (RD[3]2) depths. Below these levels, a layered cryostructure is present, overlying a suspended ice-rich zone at approximately 210 and 220 cm depths for RD[3]1 and RD[3]2, respectively (Fig. 11f). Below this last ice-rich zone, the layered structure is present, and the ice content decreases with depth. The geocryological and sedimentary profiles of the two cores are consistent, again with a gap of ~15 cm

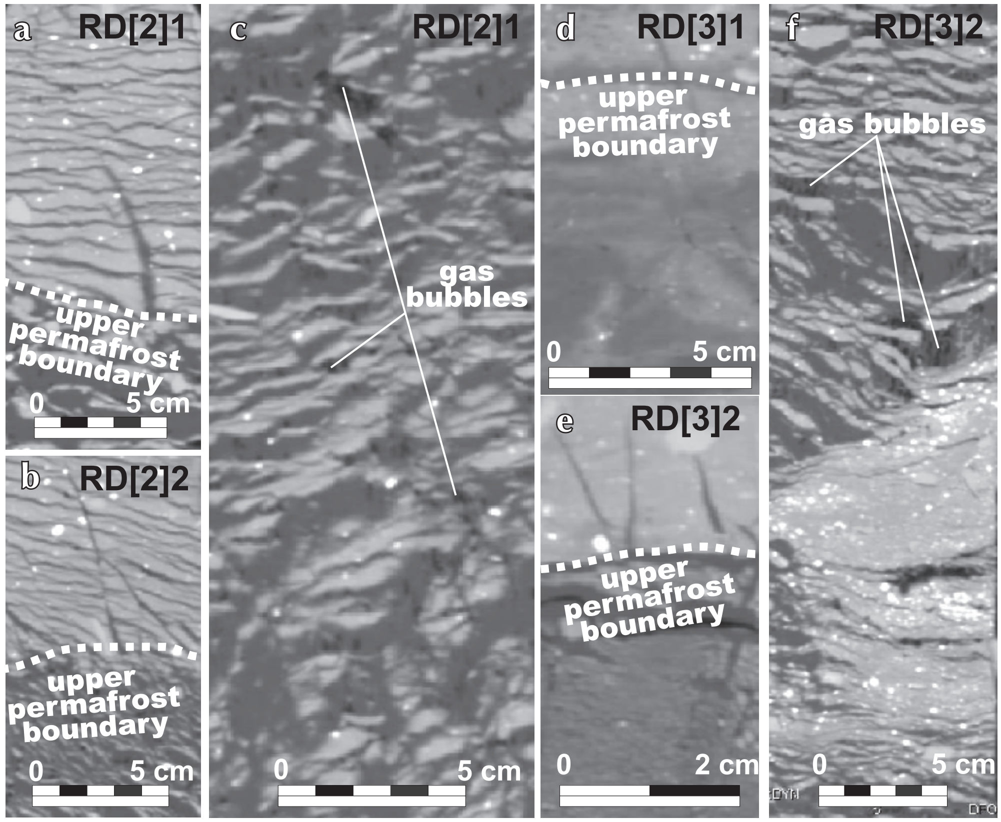

Figure 11. *Cryostructures in core RD[2]1, RD[2]2, RD[3]1, and RD[3]2 (1970s road sites). **(a)** Upper permafrost boundary overlying a suspended cryostructure (RD[2]1). **(b)** Upper permafrost boundary above suspended cryostructure (RD[2]2). **(c)** Suspended cryostructure (RD[2]1). **(d)** Upper permafrost boundary above organic-rich crysostructure (RD[3]1). **(e)** Upper permafrost boundary above organic-rich crysostructure (RD[3]2). **(f)** Suspended cryostructure (RD[3]2).*

attributable to the topographic difference between the rut and the centre mound. Similar to RD[2] cores, two ice-rich zones with suspended cryostructure are present in the RD[3] cores at 130 to 145 cm and 210 to 220 cm, but sites on road three seem to have less degradation, or a faster recovery, given the shallower active layer.

DISCUSSION

The important element that we draw attention to in these cores is the presence of the suspended cyrostructure, and its significance with respect to site history. As the suspended cryostructure is often associated with an ice-rich upper permafrost boundary, it likely marks the former top of the permafrost table following a past disturbance and recovery of the active layer.

All cores sampled near the road sites show two zones of prominent suspended cryostructure, while the forested site has only one zone. Since all of the sites have the same sedimentological setting, and are subject to the same climatic conditions, we can hypothesize that the principal factor influencing the occurrence and depth of these ice-rich layers would be the timing and nature of surface disturbances at each site. Site W1 underwent one known episode of recent perturbation with deforestation in the early 20th century associated with gold rush era development, whereas the road sites include at least two episodes, the first being the deforestation and the second in response to road clearing. Consequently, the unique ice-rich zone observed at 2 m in W1 likely reflects recovery from the early 20th century degradation. Similarly, in the road sites, the shallowest ice-rich zone was from 130 to 145 cm and reflects the recovery from the road clearing in the late 1960s to early 1970s. The deepest ice-rich zone occurring from 210 to 220 cm, is broadly similar to the W1 site, and likely reflects recovery from early 20th century deforestation.

These ice-rich layers likely reflect past episodes of permafrost degradation and recovery. These levels mainly occur when the freezing front is stationary or progresses slowly and ice segregation processes can generate a thick ice layer. These conditions of weak thermal gradient typically occur following a period of degradation, when the thawing front stagnates. Thereafter, the freezing process starts to progress upward from the permafrost table, or aggradation of the permafrost table begins.

CONCLUSION

In the last century, several perturbations of permafrost occurred at the Dominion Creek study site in response to changing surface conditions associated with early 20th century deforestation, road clearing, and more recently, a forest fire. A consistent set of observations seems to be associated with each of these disturbances. The perturbations are marked initially by a thickening of the active layer over several decades followed by the development of a suspended cryostructure as the permafrost table stabilizes, and ultimately by re-aggradation of the permafrost table as vegetation recovers from the disturbance. The timing of these changes between degradation and recovery is still not well established, but almost certainly depends on the magnitude of the disturbance, and critically, the re-establishment of vegetation cover and its insulating properties.

Vegetation cover influences ground thermal regime; for example, through changes in summer insulation (which shields permafrost from exposure to the sun), or potentially capturing additional winter snow fall (which prevents cold-temperature penetration of the ground during winter) (Linnel, 1973; Burn, 1998). The preliminary results in this study suggest variation of vegetation cover will have a stronger and more immediate impact than temperature alone. Future warming may lead to degradation of the permafrost table as ground temperatures warm and active layers increase; however, these changes will be moderated by the overlying surface cover. Results of this study suggest that some of the related permafrost dynamics can be captured through the record of past disturbances.

CT scanning is a suitable and useful method to study permafrost dynamics through detailed cryostratigraphy. This technique may be more broadly applied in Yukon as a means to document and characterize recent changes in near-surface permafrost, and to provide tangible information about the future evolution of permafrost terrain under predicted warmer climate.

ACKNOWLEDGEMENTS

We thank the Sailer family who have been mining in the study area for many decades and provided us with detailed descriptions of the history of their ground, which provided us with much of the sampling strategy that we used in this study. We particularly appreciate the help of Alberto Reyes and Chris Atkins for field assistance, and Shauna Cameron (Alberta Research Council) for operation of the CT scanner. The manuscript benefited from the constructive comments of Michel Allard (Laval University). Funding for this research was provided by a contract from the Yukon Geological Survey, in addition to the Fonds Québécois de la Recherche sur la Nature et les Technologies Fond, the Natural Sciences and Engineering Research Council of Canada, and Alberta Ingenuity New Faculty Award.

REFERENCES

Burn, C.R., 1998. The response (1958-1997) of permafrost and near-surface ground temperatures to forest fire, Takini River valley, southern Yukon Territory. Canadian Journal of Earth Sciences, vol. 35, p. 184-199.

Calmels, F. and Allard, M., 2004. Ice Segregation and Gas Distribution in Permafrost using Tomodensitometry Analysis. Permafrost and Periglacial Processes, vol. 15, p. 367-378.

Calmels, F. and Allard, M., 2008. A structural interpretation of the palsa/lithalsa growth mechanism through the use of CT Scanning. Earth Surface Processes and Landforms, vol. 33, p. 209-225.

Calmels, F., Gagnon, O. and Allard, M., 2005. A portable earth-drill system for permafrost studies. Permafrost and Periglacial Processes, vol. 16, p. 311-315.

French, H.M., 1996. The Periglacial Environment. Addison Wesley Longman, New York, 341 p.

Froese, D.G., Westgate, J.A., Reyes, A.V., Enkin, R.J. and Preece S.J., 2008. Ancient permafrost and a future warmer Arctic. Science, vol. 321, no. 5896, p. 1648.

Gilpin R.R., 1980. A Model for the Prediction of Ice Lensing and Frost Heave in Soils. Journal of Water Resources Research, vol. 16, p. 918-930.

Green, L., 1977. The gold hustlers. Alaska Northwest Publishing Company, Anchorage, Alaska, 295 p.

Hogan, B. and Skuce, G., 1992a. Klondike Mine Railway. Preliminary Survey and Field Recording Project. Dawson City Museum and Historical Society, 11 p.

Hogan, B. and Skuce, G., 1992b. North Folk Power Project. Preliminary Survey and Field Recording. Dawson City Museum and Historical Society, 14 p.

Hogan, B. and Skuce, G., 1993. Yukon Ditch. Klondike Syphon to Bonanza Creek. Preliminary Survey and Field Recording Project. Dawson City Museum and Historical Society, 11 p.

International Permafrost Association (IPA), 2005. Multi-language glossary of permafrost and related ground-ice terms. Compiled and edited by R.O. van Everdingen, Arctic Institute of North America, University of Calgary, Canada, 130 p.

Konrad J.-M., 1990. Theoretical Modelling of Massive Icy Beds. In Fifth Canadian Permafrost Conference, Université Laval, Quebec City. Nordicana, vol. 54, p. 31-35.

Linnel, K.A., 1973. Long term effects of vegetation cover on permafrost stability in an area of discontinuous permafrost. Proceedings of the Second International Conference on Permafrost, Yakutsk, USSR, North American Contribution. National Academy of Sciences, Washington, D.C., p. 688-693.

Lawrence, D.M. and Slater, A.G., 2005. A projection of severe near-surface permafrost degradation during the 21st century. Geophysical Research Letters, vol. 32, L24401.

Mackay J.R., 1971. The Origin of Massive Icy Beds in Permafrost, Western Arctic Coast, Canada. Canadian Journal of Earth Sciences, vol. 8, p. 397-422

Mackay J.R., 1972. The World of Underground Ice. Annals of the Association of American Geographers, vol. 62, no. 1, p. 1-22.

Mackay J.R., 1974. Reticulate Ice Veins in Permafrost, Northern Canada. Canadian Geotechnical Journal, vol. 11, p. 230-237.

Morse, K.T., 2003. The Nature of Gold: An Environmental History of the Klondike Gold Rush. University of Washington Press, Washington, 290 p.

Williams P.J., 1979. Propriétés générales des sols gelés. Gel des Sols et des Chaussées. Association Amicale des Ingénieurs Anciens Élèves de L'École Nationale des Ponts et Chaussées. École Nationale des Ponts et Chaussées, Paris, p. 17-19.

Williams, P.J. and Smith, M., 1995. The Frozen Earth. Fundamentals of Geocryology. Reprinted. Studies in Polar Research, Cambridge University Press, 306 p.

Yershov E.D., 1998. General Geocryology. Studies in Polar Research. Cambridge University Press, U.K., 580 p.